



# Biotic factors dominantly determine soil inorganic carbon stock across Tibetan alpine grasslands

Junxiao Pan<sup>1</sup>, Jinsong Wang<sup>1</sup>, Dashuan Tian<sup>1</sup>, Ruiyang Zhang<sup>1</sup>, Yang Li<sup>1</sup>, Lei Song<sup>1,2</sup>, Jiaming Yang<sup>1</sup>, Chunxue Wei<sup>1</sup>, and Shuli Niu<sup>1,2</sup>

<sup>1</sup>Key Laboratory of Ecosystem Network Observation and Modeling, Institute of Geographic Sciences and Natural Resources Research, Chinese Academy of Sciences, Beijing 100101, People's Republic of China

<sup>2</sup>College of Resources and Environment, University of Chinese Academy of Sciences, Beijing 100049, People's Republic of China

**Correspondence:** Jinsong Wang (wangjinsong@igsnr.ac.cn) and Shuli Niu (sniu@igsnr.ac.cn)

Received: 29 June 2022 – Discussion started: 20 July 2022

Revised: 6 October 2022 – Accepted: 11 October 2022 – Published: 28 October 2022

**Abstract.** The soil inorganic carbon (SIC) pool is a major component of soil carbon (C) pools, and clarifying the predictors of SIC stock is urgent for decreasing soil C losses and maintaining soil health and ecosystem functions. However, the drivers and their relative effects on the SIC stock at different soil depths remain largely unexplored. Here, we conducted a large-scale sampling to investigate the effects and relative contributions of abiotic (climate and soil) and biotic (plant and microbe) drivers on the SIC stock between topsoils (0–10 cm) and subsoils (20–30 cm) across Tibetan alpine grasslands. Results showed that the SIC stock had no significant differences between the topsoil and subsoil. The SIC stock showed a significant increase with altitude, pH and sand proportion, but declined with mean annual precipitation (MAP), plant aboveground biomass (PAB), plant coverage (PC), root biomass (RB), available nitrogen (AN), microbial biomass carbon (MBC), and bacterial abundance (BA) and fungal gene abundance (FA). For both soil layers, biotic factors had larger effects on the SIC stock than abiotic factors did. However, the relative importance of these determinants varied with soil depth, with the effects of plant and microbial variables on SIC stock weakening with soil depth, whereas the importance of climatic and edaphic variables increased with soil depth. Specifically, BA, FA and PC played dominant roles in regulating SIC stock in the topsoil, while soil pH contributed largely to the variation of SIC stock in the subsoil. Our findings highlight differential drivers over SIC stock with soil depth, which should be considered in biogeochemical models for better simulating and predicting SIC dynamics and its feedbacks to environmental changes.

## 1 Introduction

Soils store approximately 1500 Pg of organic carbon (SOC) and 940 Pg of inorganic carbon (SIC) to a depth of 1 m (Batjes, 1996; Jobbágy and Jackson, 2000), which are the largest carbon (C) pool in the terrestrial ecosystem and play a critical part in the global C cycling (Darwish et al., 2018; Lal, 2004; Prietzel et al., 2016). To alleviate the elevated levels of atmospheric carbon dioxide (CO<sub>2</sub>), most previous studies concentrate on the SOC pool because it responds quickly to global climate change such as warming and nitrogen (N)

deposition, and it is strongly linked with various ecosystem functions (Wang et al., 2002; Yang et al., 2012). Compared to the relatively short turnover time of SOC, SIC has a long residence time due to soil weathering (Monger et al., 2015; Zang et al., 2018), which is considered to be fairly stable and has less contribution to changes in terrestrial ecosystem C balance (Yang et al., 2012). Therefore, previous studies have paid little attention to SIC. However, recent studies suggest that SIC is also responsive to anthropogenic activities and global climate changes such as soil acidification, atmospheric N deposition, and global warming (Yang et al., 2010;

Song et al., 2022), acting as a critical C source (Liu et al., 2020) or C sink (Gao et al., 2018; Liu et al., 2021). Thus, the preservation of SIC and its roles in climate mitigation should not be neglected, especially in arid and semiarid grasslands which store a large amount of SIC (Yang et al., 2012).

The SIC stock and stability can be fundamentally altered by an array of abiotic and biotic processes (Raza et al., 2020). High precipitation can promote the weathering of soil silicate minerals and removal of base cations ( $\text{Ca}^{2+}$ ,  $\text{Mg}^{2+}$ ,  $\text{K}^{+}$  and  $\text{Na}^{+}$ ) by leaching (Vicca et al., 2022). Soil acidification due to atmospheric nitrogen (N) and acid deposition and the nitrification of  $\text{NH}_4^{+}$  may greatly accelerate soil carbonate dissolution and  $\text{CO}_2$  releases (Raza et al., 2020; Song et al., 2022). Plant growth can deplete soil carbonates by releasing proton and organic acids from root rhizosphere (Goulding, 2016; Kuzyakov and Razavi, 2019), and biological  $\text{N}_2$  fixation by some legumes are likely to cause SIC losses (Tang et al., 1999). Furthermore, plant autotrophic and microbial heterotrophic respiration often facilitate carbonate dissolution by enhancing  $\text{CO}_2$  partial pressures (An et al., 2019; Liu et al., 2021). Nevertheless, how these abiotic and biotic factors affect SIC stock and what the relative importance is of these confounding drivers remain largely uncertain.

Previous studies on SIC stock have mostly focused on the topsoil within 10 cm soil depth (Yost and Hartemink, 2020), which are relatively different from the subsoil (i.e., soils residing > 20 cm below ground) in the aspect of biochemical processes, plant roots, soil properties, and microbial communities (Rumpel et al., 2012; Zhou et al., 2021), while the patterns of SIC stock in the subsoil on a large scale remain elusive. The predictors of SIC stock in the subsoil may differ from those in the topsoil due to distinct soil microenvironments, soil physicochemical properties, root exudates, and microbial abundance and functions (Jia et al., 2017). For instance, the topsoil has larger root biomass (RB) and higher microbial activity than the subsoil, but the subsoil tends to preserve soil parent material because of the weakened weathering by the isolation of heat and energy from the surface soil (Crowther et al., 2016). Thus, the abiotic and biotic variables may exhibit different effects on SIC stock in the subsoil compared to the topsoil due to the various importance of these variables.

The Tibetan Plateau has the largest alpine grassland on the Eurasian continent, which is a vital component of global terrestrial ecosystems, providing an ideal platform to explore SIC stock and its determinants (Wang et al., 2002; Yang et al., 2010). During the past several decades, the plateau has experienced significant warming (Wang et al., 2008) and pronounced atmospheric N deposition (Liu et al., 2013; Yu et al., 2019). This continuous warming and N deposition have resulted in a significant increase in plant growth and soil acidification (Ding et al., 2017; Yang et al., 2012), which could likely induce potential  $\text{CO}_2$  releases from soil carbonates by biogeochemical processes (Raza et al., 2020). However, a

general understanding of SIC stock with soil depth across Tibetan alpine grasslands remains unexplored.

Here, we researched the relative importance of climatic, edaphic, plant and microbial variables to SIC stock at different soil layers along an approximately 3000 km transect of alpine grasslands on the Tibetan Plateau, spanning a broad range of climatic and geographical conditions. Specifically, two key questions are addressed in this study: (1) What are the differences of SIC stock between the topsoil and subsoil? (2) What is the relative importance of climatic, edaphic, plant and microbial variables to the variation of SIC stock along with soil depth?

## 2 Materials and methods

### 2.1 Study area and field sampling

From 30 July to 28 August 2020, we conducted large-scale systematic field surveys and samplings in Tibetan alpine grasslands. The total 25 sampling sites covered approximately 3000 km and included three grassland types (i.e., 11 alpine meadow, 8 alpine steppe, and 6 alpine desert sites). The distance between nearby sampling sites was about 120 km. The study sites cover a broad geographic and climatic range, with longitude and latitude ranging from  $79^{\circ}49'39''$  to  $102^{\circ}25'31''$  E and  $31^{\circ}06'37''$  to  $32^{\circ}43'09''$  N, respectively, and the altitude ranging from 3500 to 5016 m. These sites covered a broad precipitation gradient varying between 72 and 706 mm. The mean annual temperature (MAT) ranged from  $-3.9$  to  $5.8^{\circ}\text{C}$ . The plant communities were dominated by *Kobresia tibetica* Maxim, *Stipa caucasica*, *Kobresia pygmaea*, *Stipa purpurea*, and *Leontopodium pusillum*. Soils were Cambisol and some were loess-derived Luvisol. The site location, grassland type, climatic, and plant parameters are detailed in Table S1 in the Supplement.

### 2.2 Climatic data

The climatic data were derived from the Loess Plateau Scientific Data Center (LPSDC, <http://loess.geodata.cn/>, last access: 25 October 2022) (Peng et al., 2019). The Kriging interpolation was conducted to obtain spatial distributions of 30-year (1987–2017) MAT and mean annual precipitation (MAP) at each sampling site by a geographic coordinate system.

### 2.3 Soil properties

At each site, we selected four  $1\text{ m} \times 1\text{ m}$  plots for soil and plant samplings and the distance between nearby sampling plots was 25 m. In each plot, a 7.5 cm diameter soil drill was used to take five soil cores at fixed soil depths (0–10, 10–20, and 20–30 cm), and a 2 mm mesh was used to remove stones. Based on our field observation, the soil depth is relatively shallow (less than 40 cm) for alpine grasslands, es-

pecially for the alpine desert. Moreover, most of the below-ground roots in alpine grasslands distribute on the surface of 10 cm and decrease sharply below 20 cm. Thus, we defined the topsoil and subsoil as 0–10 and 20–30 cm soils, respectively. After mixing, 100 g of fresh soils from each plot were collected and stored in a  $-4^{\circ}\text{C}$  portable icebox, then returned to the laboratory and stored at  $-20^{\circ}\text{C}$  for microbial properties. The rest of the soil samples, about 700 g, were also sent back to the laboratory and air-dried for measurements of other soil properties including soil pH, available nitrogen (AN), and mechanical composition. A  $40\text{ cm} \times 40\text{ cm} \times 40\text{ cm}$  (length  $\times$  width  $\times$  depth) pit was dug for measuring soil bulk density (BD) by using a constant volume soil-sampling drill ( $100\text{ cm}^3$ ), and the undisturbed soil was preserved in aluminum specimen boxes, returned to the laboratory and oven-dried for 48 h at  $105^{\circ}\text{C}$  and weighed. The oven-dried soil (20 g) was screened for gravel by sifting through a 2 mm mesh sieve and materials larger than 2 mm were collected and weighed to determine the percentage of gravels. Soil pH (1 : 25 soil :  $\text{H}_2\text{O}$ ) was measured using a soil pH meter, and AN was determined by the alkaline-hydrolysis diffusion method. A laser particle analyzer (Mastersizer 2000, Malvern Panalytical, UK) was applied to measure soil mechanical compositions, including the proportion of clay ( $< 2\text{ }\mu\text{m}$ ), silt ( $2\text{--}50\text{ }\mu\text{m}$ ), and sand ( $> 50\text{ }\mu\text{m}$ ). The SIC was determined by using an inorganic C elemental analyzer (multi EA<sup>®</sup> 4000; Analytic Jena, Germany). The multi EA 4000 C elemental analyzer was equipped with the automatic total inorganic carbon (TIC) solids module and calibrated before the analysis. The sample boat was acidified automatically with 40 %  $\text{H}_3\text{PO}_4$  in the reactor of the TIC module. The  $\text{CO}_2$  from the carbonate was released, the measuring gas was dried and cleaned and the carbon content was measured by means of the wide-range nondispersive infrared sensor (NDIR) detector. Before being analyzed directly, all soil samples were ground into solid fine powders with a mortar, and for the determination of TIC, a standard, prepared by the dilution of the solids  $\text{CaCO}_3$  with  $\text{SiO}_2$  (0.2 % C), was used, with a weighting range of 7–200 mg, to cover a wide concentration range.

## 2.4 Plant properties

In each plot, we estimated plant coverage (PC) by the projection method, namely the proportion of vegetation projection to the area of the sampling plot. In addition, plant above-ground biomass (PAB) was clipped to ground level and collected, belowground roots were sampled by three soil samples in each plot which were mixed by two soil cores with a 7.5 cm diameter drill and collected from soil by rinsing them in water. Finally, they were oven-dried at  $60^{\circ}\text{C}$  and weighed to determine PAB and RB, respectively.

## 2.5 Microbial attributes

Soil microbial biomass carbon (MBC) was measured by using a chloroform fumigation–extraction procedure (Brookes et al., 1985). Briefly, 10 g of unfumigated and chloroform-fumigated fresh soil samples were extracted by using 0.5 M  $\text{K}_2\text{SO}_4$  after 24 h of incubation, respectively. Then, the extracts were analyzed by using a total organic carbon (TOC) analyzer (multi N/C<sup>®</sup> 3100; Analytic Jena, Germany). The MBC was determined by the differences in C concentrations between unfumigated and chloroform-fumigated samples, and the correction factor (i.e.,  $\text{KC} = 0.45$ ) was used to convert microbial C to MBC (Joergensen, 1996).

Real-time polymerase chain reaction (qPCR) was used to quantify bacterial abundance (BA) and fungal gene abundance (FA) by the absolute quantification method based on the gene copy number (Tatti et al., 2016). Each reaction was carried out 3 times with a mixture of a total  $20\text{ }\mu\text{L}$  volume, including  $2\text{ }\mu\text{L}$  of DNA template,  $10\text{ }\mu\text{L}$  of  $2 \times \text{ChamQ SYBR Color qPCR Master Mix}$ , and  $0.4\text{ }\mu\text{L}$  ( $5\text{ }\mu\text{M}$  concentration) each of forward and reverse primer, specific for each gene; and the qPCR conditions were  $95^{\circ}\text{C}$  for 5 min, then 40 cycles for the 18S rRNA (ribosomal ribonucleic acid) gene and 16S rRNA gene. Each cycle involved melting at  $95^{\circ}\text{C}$  for 30 s, annealing at  $55^{\circ}\text{C}$  for 30 s, an extension of  $72^{\circ}\text{C}$  for 40 s, and finally  $10^{\circ}\text{C}$  until terminated. The primer pair SSU0817/1196 and Eub338/Eub806 were used for amplifying fungi and bacteria in qPCR amplification, respectively. Finally, the DNA concentration was determined by using a QuantiFluor<sup>TM</sup>-ST fluorescent quantitative system (Promega, Fitchburg, WI, USA). The abbreviations of all variables were detailed in Table S2.

## 2.6 Statistical analyses

The total SIC density (C stock per land area) in each soil-depth layer was calculated using Eq. (1) (Pan et al., 2019):

$$\text{SIC density (g C m}^{-2}\text{)} = \text{SIC (g C kg}^{-1}\text{)} \times \text{BD (g cm}^{-3}\text{)} \times d \text{ (cm)} \times (1 - g)/100, \quad (1)$$

where SIC is the soil inorganic C content,  $d$  is the depth of the soil layer (0.1 m), BD is bulk density, and  $g$  is the percentage of gravel fraction ( $> 2\text{ mm}$ ).

First, the differences of SIC stock and corresponding abiotic and biotic variables between the topsoil and subsoil were examined by  $T$ -test. Second, SIC density and various abiotic and biotic variables were log-transformed and standardized ( $Z$ -score normalization) to perform the assumption of normality and homogeneity by the Shapiro–Wilk test and Levene's test, respectively (Pan et al., 2021). Then, the linear regressions were used to test SIC density with different variables for both the topsoil and subsoil across sites. Also, the Pearson correlation coefficients between SIC density and each variable are analyzed in Table S3.

Third, a linear model (lm) was employed to examine SIC density with abiotic and biotic variables by using the maximum likelihood estimation with the lm package. The relative effect of all parameter estimates was calculated to evaluate the relative importance of drivers in predicting SIC density. Each predictor variable was simultaneously tested in the model, which was comparable for the contribution of different types of predictor factors to SIC density. The absolute values of standardized regression coefficients of the explanatory variables accounting for the percentage of the sum of all standardized regression coefficients were used to express the importance of predictors (Gross et al., 2017; Le Provost et al., 2020). Also, SIC density and abiotic and biotic variables were standardized before analyses using the Z-score to interpret variable estimates on a comparable scale (Gross et al., 2017):

$$\log(\text{SIC density}) = \beta_0 + \beta_1 \log X_1 + \beta_2 \log X_2 + \dots + \beta_{12} \log X_{12} \quad (2)$$

where  $\beta_0$  and  $\beta_i$  ( $i = 1, 2, 3 \dots 12$ ) are intercept and coefficients, respectively. To explore the predictors of SIC density in different soil depths across all sites, the absolute values of slopes of the variables were extracted and plotted. Then, to quantify their relative contribution to SIC density, 12 predictor variables were categorized into 4 groups, including climatic (MAP, MAT and altitude), edaphic (pH, AN and sand proportion), plant (PB, PC and RB), and microbial (MBC, BA and FA) factors. The detailed categorization of explanatory variables is listed in Table S2.

Furthermore, the relative importance of abiotic (climatic and edaphic) and biotic (plant and microbial) variables in predicting SIC density was quantified by performing variation partitioning analyses (VPAs; Borcard et al., 1992) and using the “vegan” package in R 4.1.3 which was used to divide the variation of SIC density among two types of explanatory variables for their individual and joint effects. In this analysis, the common and unique contribution of sets of explanatory variables (two sets including abiotic and biotic variables) in SIC density is determined. Additionally, the residuals were determined by a fraction of variations in response variables, which could not be explained by any of the explanatory variables. The VPA method allows us to explore the variation clearly by the percentage of explanatory variables, which are easy to interpret and can be discussed in the context of SIC density.

### 3 Results

#### 3.1 SIC density and influencing variables in different soil depths

The SIC density and SIC content had no significant differences between the topsoil and subsoil, but the BD in the subsoil was much higher compared with the topsoil. Specifically, SIC density in the topsoil and subsoil ranged from 1.8

to 3271 and 5.4 to 3214 g C m<sup>-2</sup> across 25 sampling sites, with an average of  $802 \pm 220$  and  $814 \pm 236$  g C m<sup>-2</sup>, respectively (Fig. 1). No significant changes in SIC density with soil depth were observed in both the alpine steppe and alpine desert ( $p = 0.113$  and  $p = 0.068$ , respectively; Fig. 1) sites, but SIC density was higher in the subsoil than that in the topsoil in the alpine meadow ( $p = 0.002$ , Fig. 1).

Meanwhile, the majority of abiotic and biotic drivers had significant differences between the topsoil and subsoil (Table 1). The RB, AN, MBC, BA, and FA in the topsoil were significantly larger than those in the subsoil (all  $p < 0.001$ ). In contrast, pH was significantly lower in the topsoil than in the subsoil ( $p < 0.001$ , Table 1). However, the sand proportion between the two soil depths had no significant differences (Table 1).

#### 3.2 Associations of SIC density with abiotic and biotic variables

The SIC density was closely related to multiple abiotic and biotic variables (Table S3, Figs. 2 and 3 for topsoil and subsoil, respectively). For both the topsoil and subsoil, the SIC density showed a significant increasing trend with altitude, pH, and sand proportion, but declined with MAP, PAB, PC, RB, AN, BA and FA (all  $p < 0.05$ ). The SIC density showed a correlation with MBC in the topsoil ( $p < 0.05$ , Fig. 2) but not in the subsoil (Fig. 3). Meanwhile, the SIC density in both soil depths did not significantly correlate with MAT (Figs. 2 and 3). In addition, the absolute value of slope for the regression equation for the most explanatory variables (except for AN, MAT and MBC) in the topsoil was larger than that of the subsoil, especially for RB and sand proportion (Figs. 2 and 3).

#### 3.3 Determinants of SIC density in different soil depths

The linear model and VPA collectively showed that the predominant predictors of SIC density differed with soil depth (Figs. 4 and 5). Specifically, for the topsoil, the linear model revealed that microbial and plant variables largely explained the variations in the SIC density, followed by edaphic variables, and climate contributed the least (Fig. 4). Among these variables, PC, BA and FA exhibited larger effects on the SIC density compared with other predictor factors (Fig. 4). Moreover, the VPA illustrated that biotic factors explained the majority variation of SIC density compared with abiotic factors (Fig. 5). For the subsoil, the linear model showed that edaphic variables largely explained the variation in SIC density, followed by microbial and plant variables, and climate contributed the least (Fig. 4). Among these variables, the soil pH had larger contributions to the variation of SIC density than others (Fig. 4). Meanwhile, the VPA confirmed that the predictions of biotic factors on SIC density were better than those of abiotic factors in the subsoil (Fig. 5).



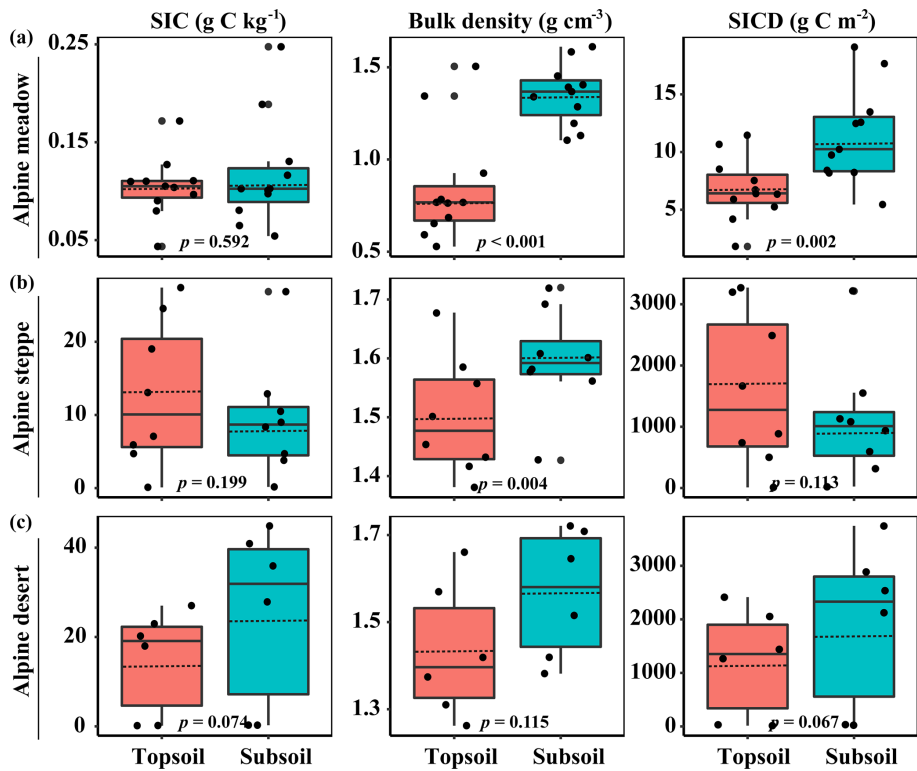


**Figure 1.** Soil inorganic C (SIC) content, bulk density (BD), and SIC density (SICD) in the topsoil and subsoil. The horizontal solid and hollow lines inside each box represent medians and mean values, respectively. Significant differences between the topsoil and subsoil were inspected according to Tukey’s test.

**Table 1.** Edaphic, plant and microbial properties between the topsoil and subsoil for 25 sampling sites.

Parameters	Topsoil	Subsoil	<i>p</i> value
RB (g m <sup>-2</sup> )	1670 ± 359	95.2 ± 15.3	< 0.001
pH	7.66 ± 0.28	7.85 ± 0.26	< 0.001
AN (mg kg <sup>-1</sup> )	217 ± 43.7	131 ± 22.0	0.004
SP (%)	47.1 ± 4.33	45.6 ± 4.87	0.698
MBC (mg kg <sup>-1</sup> )	385 ± 73.8	101 ± 9.7	0.001
BA (10 <sup>9</sup> gene copies g <sup>-1</sup> soil)	27.2 ± 5.68	12.6 ± 2.86	0.001
FA (10 <sup>7</sup> gene copies g <sup>-1</sup> soil)	14.2 ± 3.25	3.62 ± 0.84	0.001

RB: root biomass; AN: soil available nitrogen; SP: sand proportion; MBC: microbial biomass carbon; BA: soil bacterial abundance; FA: soil fungal abundance. Values are means ± standard error (SE); *p* values represent significant differences between the topsoil and subsoil according to Tukey’s test.

#### 4 Discussion

To the best of our knowledge, this study was the first to study large-scale evidence of the relative contribution of abiotic and biotic drivers to the variation of SIC stock at different soil depths, which has considerable implications for grasping the importance of SIC in the ecosystem C cycling. Due to considerably stable characteristics and the long turnover time (Mi et al., 2008; Yang et al., 2010; Zamanian et al., 2018), SIC stock is traditionally considered to be dominated by abiotic factors including soil moisture, soil pH,

CO<sub>2</sub> partial pressure, and Ca<sup>2+</sup> concentrations according to the equilibrium of carbonate precipitation–dissolution reactions ( $\text{CaCO}_3 + \text{H}_2\text{O} + \text{CO}_2 \rightarrow \text{Ca}^{2+} + 2\text{HCO}_3^-$  and  $\text{Ca}^{2+} + 2\text{HCO}_3^- \rightarrow \text{CaCO}_3 + \text{H}_2\text{O} + \text{CO}_2$ ) and mineral carbonation ( $\text{MgSiO}_4 + 2\text{CO}_2 \rightarrow 2\text{MgCO}_3 + \text{SiO}_2$  and  $\text{CaMgSi}_2\text{O}_6 + \text{CO}_2 + \text{H}_2\text{O} \rightarrow \text{Ca}_2\text{Mg}_5\text{Si}_8\text{O}_{22}(\text{OH})_2 + \text{CaCO}_3 + \text{SiO}_2$ ) (Mi et al., 2008; Rey, 2015; Yang et al., 2012; Yang and Yang, 2020). These abiotic factors were proved to have large impacts on the dissolution and deposition processes of inorganic C and ultimately determined the

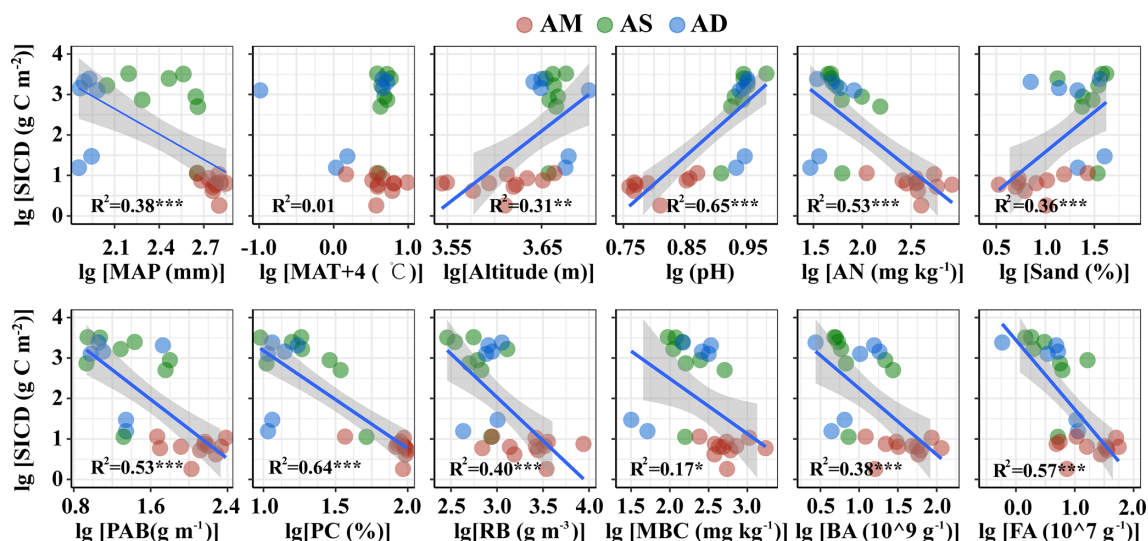


**Figure 2.** SIC density in relation to climatic, edaphic, plant and microbial factors in the topsoil. The solid lines are fitted by ordinary least-squares regressions, and the shadow areas correspond to 95 % confidence intervals. AM: alpine meadow; AS: alpine steppe; AD: alpine desert; MAP: mean annual precipitation; PAB: plant aboveground biomass; PC: plant coverage. The abbreviations for other variables are shown in Table 1. \*  $p < 0.05$ ; \*\*  $p < 0.01$ ; \*\*\*  $p < 0.001$ .

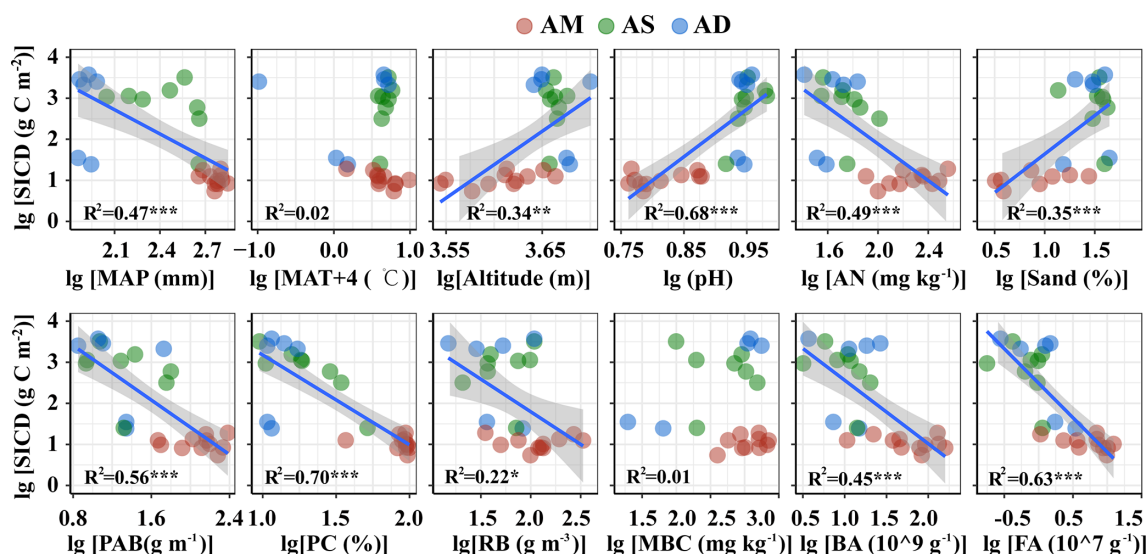


**Figure 3.** SIC density in relation to climatic, edaphic, plant and microbial factors in the subsoil. The solid lines are fitted by ordinary least-squares regressions, and the shadow areas correspond to 95 % confidence intervals. AM: alpine meadow; AS: alpine steppe; AD: alpine desert.

reservation and distribution of SIC (Rey, 2015; Rowley et al., 2018).

However, many biological processes and factors were not quantitatively considered in previous studies. In this study, based on the approach of large-scale field samplings across Tibetan alpine grasslands, we estimated the predominant drivers of SIC stock in the topsoil and subsoil. Our results found the predominant roles of microbial and plant factors in determining SIC stock in both topsoil and subsoil. More importantly, the effects of biotic factors on SIC stock weak-

ened with soil depth (Fig. 4). These results were different from those demonstrating the critical influence of abiotic processes on SIC stock (Mi et al., 2008; Yang et al., 2010).

We found that SIC density showed a declining trend with the increasing plant aboveground biomass, plant coverage, and root biomass (Figs. 2 and 3). Plant factors could contribute to the decline of SIC stock by three pathways including uptakes of exchangeable cations, plant organic matter inputs, and rhizosphere processes. First, a large decline in soil base cations is likely to be induced by plant uptake with in-

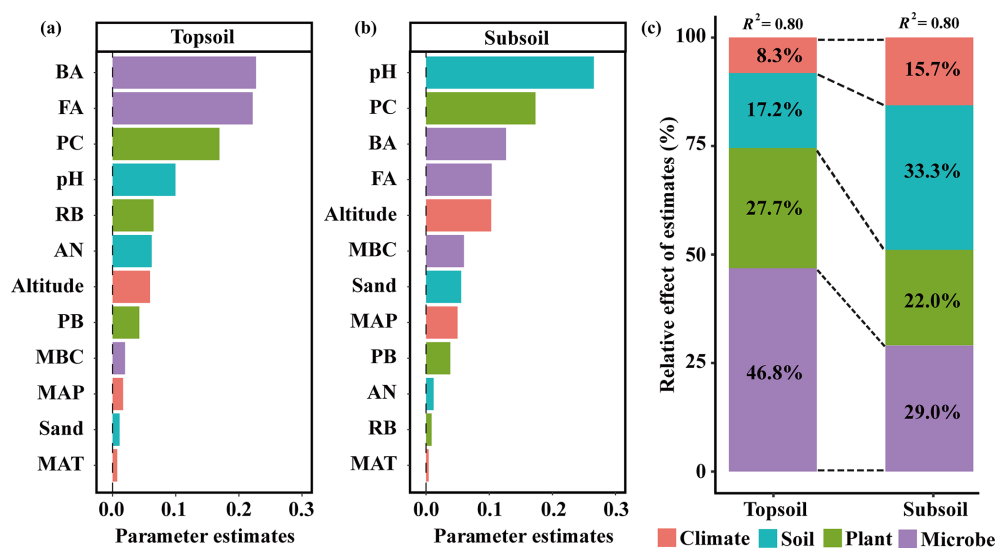


**Figure 4.** Relative effects of multiple drivers of SIC density in the (a) topsoil and (b) subsoil. Climatic variables include MAP, MAT and altitude; edaphic variables include pH, AN and sand proportion; plant variables include PB, PC and RB; microbial variables include MBC, BA and FA.

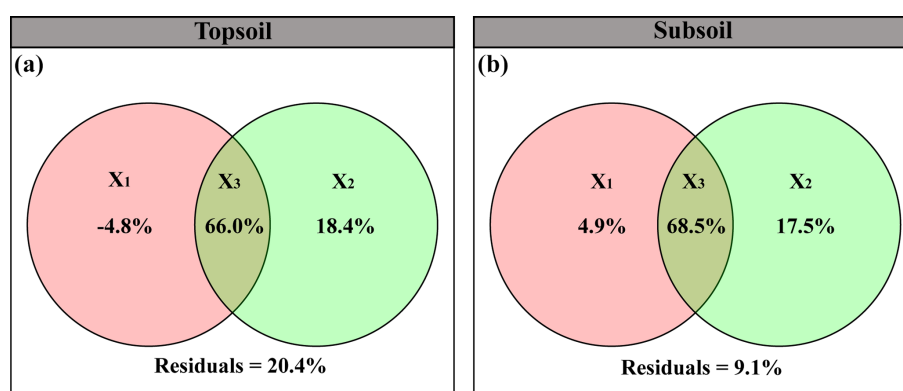


**Figure 5.** Variation partitioning analyses (VPAs) reveal the relative contribution of abiotic and biotic variables to SIC density in the (a) topsoil (61.2 % vs. 84.4 %) and (b) subsoil (73.4 % vs. 86.1 %), respectively. Results in three fractions: the unique effect of abiotic factors (X1), the unique effect of biotic factors (X2), and common interception of abiotic and biotic factors (X3).

creasing plant biomass; and the losses of soil exchangeable base cations can cause the transformation of SIC to  $\text{CO}_2$ , which is ultimately released into the atmosphere (Huang et al., 2015). Second, increasing plant residue inputs can enhance carbonic and organic acid production into soil water solutions via microbial decomposition, which reduces the availability of soil base cations through cation exchange in the soil (Sartori et al., 2007) and increases the dissolution and leaching of carbonates, resulting in a decrease in the SIC. Third, the plant rhizosphere effect on releasing  $\text{CO}_2$  from carbonates should not be ignored, especially in alkaline soils. By releasing organic acids and protons as well as  $\text{CO}_2$ , plant roots can reduce soil pH and increase  $\text{CO}_2$  in the rhizosphere (Lenzowski et al., 2018), both of which dissolve carbonates by neutralization (Harley and Gilkes, 2000). In addition, or-

ganic compounds from plant root exudates, such as malate or citrate, can stimulate mineral weathering by dissolving silicate minerals (Dontsova et al., 2020).

Furthermore, the topsoil has a larger quantity and higher quality of plant residues than the subsoil, which indicates a greater potential for carbonate dissolution by biological processes for the surface soil (Liu et al., 2020). The large root biomass in the topsoil can increase the uptake of base cations and result in increasing proton and organic acids in root exudates (Li et al., 2007), thus reducing the soil carbonate content for maintaining the charge balance. In addition, the larger plant roots exuded more organic compounds in the topsoil that can stimulate parent mineral weathering and dissolve silicate minerals by chelating reaction products (Doetterl et al., 2018; Dontsova et al., 2020).

Also, the SIC density in both soil depths appears to have an increasing or decreasing trend from the alpine meadow to the alpine steppe and alpine desert (Figs. 2 and 3) sites. In the present study, for example, the alpine meadow has larger plant productivity than the alpine steppe, which implies that more plant above- and belowground residues are deposited in alpine meadow soils compared to alpine steppe soils. Therefore, from the perspective of the whole ecosystem, the grassland type would be a better predictor for the quantity and distribution of SIC density.

Previous studies reported that microbial properties may not be important in mediating SIC accumulation (Liu et al., 2021; Wang et al., 2015). However, our results found that microbial factors including microbial biomass and bacterial and fungal gene abundance showed significant associations with SIC stock (Figs. 2 and 3), which could be due to microbes driving the carbonate dissolution processes, including microbial respiration, organic matter mineralization, and releases of proton and organic acids by microbial metabolic activity. First, the increase in microbial respiration can improve CO<sub>2</sub> production and enhance the partial pressure of CO<sub>2</sub>, leading to a decline in pH and further dissolution of carbonates (Chang et al., 2012). In addition, soil organic matter mineralization and litter decomposition by microbes can induce the dissolution of CO<sub>2</sub> and the release of organic acids (Goulding, 2016; Kuzyakov and Razavi, 2019), both of which decrease the SIC stock. Meanwhile, chelates and enzymes excreted by microbes may contribute to enhancing mineral dissolution rates and organic matter decomposition (Xiao et al., 2015; Zaharescu et al., 2020).

We also revealed that bacterial and fungal gene abundance were significantly correlated with SIC stock (Figs. 2 and 3), which was likely to account for decreasing soil pH in the involvement of microbial biological reactions. For instance, nitrifying bacteria can oxidize ammonium to nitrate ( $\text{NH}_4^+ + \text{OH}^- + 2\text{O}_2 \rightarrow \text{NO}_3^- + 2\text{H}_2\text{O} + \text{H}^+$ ), and the increase in acidity is finally neutralized through accelerating carbonate dissolution (Zamanian et al., 2016). Also, some nitrogen-fixing bacteria that lived in symbiosis with leguminous plants can acidify the soil by excreting protons during N<sub>2</sub> fixation (Vicca et al., 2022). Furthermore, fungi are likely to accelerate carbonate neutralization by exuding protons and organic acids (van Hees et al., 2006; Wild et al., 2021).

Microbial factors could also be better predictors for SIC stock in the topsoil than in the subsoil. The large plant residues incorporated into the topsoil provided substantial amounts of organic matter for microbial living and decomposition (Oelkers et al., 2015; Ven et al., 2020), which can stimulate microbial abundance and activities and promote microbial extracellular enzymes. These extracellular excretions play a fundamental role in microbial respiration and CO<sub>2</sub> production, both of which stimulate silicate weathering and carbonate dissolution (Vicca et al., 2022). Meanwhile, the higher CO<sub>2</sub> flux and CO<sub>2</sub> partial pressure resulting from the biological activities of roots and soil microorganisms in

the topsoil could enhance carbonate dissolution and formations of pedogenic inorganic C (Chang et al., 2012; Zamanian et al., 2016).

Different from plant and microbial factors, the prediction of edaphic factors on SIC stock strengthened with soil depth, with soil pH being the most important predictor among edaphic variables (Fig. 4). The buffering capacity in soil solutions determines the equilibrium of ion inputs and outputs by soil pH (Huang et al., 2015). In this study, soil pH in the subsoil (7.85) was much higher than that in the topsoil (7.66) (Table 1). The higher pH could buffer the replacement of the exchangeable cations with protons (Frank and Stuanes, 2003) and increase the preservation of base cations (Gandois et al., 2011). Given that base cations and carbonates provide the major buffering capacity in the alkaline soil (Yang et al., 2012), the topsoil could be subject to a larger loss of base cations and SIC due to the lower soil pH compared to the subsoil.

Taken together, our results revealed that SIC stock was closely linked with biotic factors, which highlights the roles of biological processes in predicting SIC dynamics (Hong et al., 2019). These results imply that the widespread enhancement of vegetation productivity under global environmental changes (e.g., warming and rewetting) (Ding et al., 2017; Wang et al., 2008) may aggravate the depletion of SIC stock (Raza et al., 2020). Meanwhile, previous studies have urged the need for incorporating microbial processes and indicators into Earth system models (ESMs) to reduce the uncertainty in predicting soil C dynamics, especially SOC decomposition (Allison et al., 2010; Moorhead and Sinsabaugh, 2006; Todd-Brown et al., 2013). However, our findings highlighted the vital role of microbial factors in regulating soil C balance from inorganic C preservation. Thus, incorporating microbial processes into the models can aid the understanding of overall soil C responses, because SOC and SIC are formed, protected, and lost in different ways.

More importantly, the predictions of biotic factors on SIC stock weakened with soil depth, which implies that SIC may be susceptible to environmental changes in the topsoil which is the hotspot of root and microbial activities. Even though biotic factors in the subsoil played a less important role in predicting SIC stock compared with the topsoil, an increase in rooting depth is expected in response to climate warming and land-use change (Liu et al., 2018), which is likely to cause SIC losses in the deep soil by root growth. Therefore, it is a necessity to further explore the effects of biotic factors on SIC stock in the deep soil in the context of global changes. Although most of the variations in SIC density were explained by our measured explanatory variables, some other potential variables may also predict SIC density (Fig. 5). Then, understanding the effects of other potential abiotic and biotic factors on SIC density with soil depth is urgently needed when predicting the response and feedback of SIC to climate change in the future. Overall, the contribution of SIC to CO<sub>2</sub> is not ignored and SIC maintenance



has a considerable effect on soil C losses and is important to maintain the health and ecosystem functions (Raza et al., 2020; Zamanian et al., 2018). Our study provides robust evidence that biotic factors are correlated with SIC stock in the Tibetan plateau and that topsoils and subsoils should be considered separately when modeling SIC dynamics and its feedbacks on climate change (Yang et al., 2012; Zamanian and Kuzyakov, 2019).

## 5 Conclusions

Our findings showed that SIC stock had no significant differences between the topsoil and subsoil in the Tibetan grasslands; the climatic, edaphic, plant and microbial variables jointly predicted SIC stock in the Tibetan grasslands; and the biotic factors had a larger contribution than abiotic factors to the variation of SIC stock. Furthermore, the relative importance of explanatory variables to the variation of SIC stock varied with soil depth, the predictions of microbial and plant variables on SIC stock weakened with soil depth, while the predictions of edaphic variables strengthened with soil depth. Our results revealed that biotic factors should be considered seriously for predicting SIC stock due to their regulating roles in biological processes. The contrasting responses and drivers of SIC stock between the topsoil and subsoil highlight differential mechanisms underlying SIC preservation with soil depth, which is crucial to understanding and predicting SIC dynamics and its feedbacks to environmental changes.

**Data availability.** The data that support the findings of this study are available from the corresponding author upon reasonable request.

**Supplement.** The supplement related to this article is available online at: <https://doi.org/10.5194/soil-8-687-2022-supplement>.

**Author contributions.** JP, JW and SN designed the study. JP, JW, DT, RZ, YL, LS, JY, CW and SN were involved in drafting and revising the manuscript. All authors read and approved the final manuscript.

**Competing interests.** The contact author has declared that none of the authors has any competing interests.

**Disclaimer.** Publisher's note: Copernicus Publications remains neutral with regard to jurisdictional claims in published maps and institutional affiliations.

**Financial support.** This study was financially supported by the Second Tibetan Plateau Scientific Expedition and Research (STEP) program (grant no. 2019QZKK0302), the National Natural Science Foundation of China (grant nos. 31988102 and 32101390), and the China National Postdoctoral Program for Innovative Talents (grant no. BX20200330).

**Review statement.** This paper was edited by Marta Dondini and reviewed by Enrico Balugani and one anonymous referee.

## References

- Allison, S. D., Wallenstein, M. D., and Bradford, M. A.: Soil-carbon response to warming dependent on microbial physiology, *Nat. Geosci.*, 3, 336–340, <https://doi.org/10.1038/NGEO846>, 2010.
- An, H., Wu, X. Z., Zhang, Y. R., and Tang, Z. S.: Effects of land-use change on soil inorganic carbon: A meta-analysis, *Geoderma*, 353, 273–282, <https://doi.org/10.1016/j.geoderma.2019.07.008>, 2019.
- Batjes, N. H.: Total carbon and nitrogen in the soils of the world, *Eur. J. Soil Sci.*, 47, 151–163, <https://doi.org/10.1111/j.1365-2389.1996.tb01386.x>, 1996.
- Borcard, D., Legendre, P., and Drapeau, P.: Partialling out the spatial component of ecological variation, *Ecology*, 73, 1045–1055, <https://doi.org/10.2307/1940179>, 1992.
- Brookes, P. C., Landman, A., Pruden, G., and Jenkinson, D. S.: Chloroform fumigation and the release of soil-nitrogen – A rapid direct extraction method to measure microbial biomass nitrogen in soil, *Soil Biol. Biochem.*, 17, 837–842, [https://doi.org/10.1016/0038-0717\(85\)90144-0](https://doi.org/10.1016/0038-0717(85)90144-0), 1985.
- Chang, R. Y., Fu, B. J., Liu, G. H., Wang, S., and Yao, X. L.: The effects of afforestation on soil organic and inorganic carbon: A case study of the Loess Plateau of China, *Catena*, 95, 145–152, <https://doi.org/10.1016/j.catena.2012.02.012>, 2012.
- Crowther, T. W., Todd-Brown, K., Rowe, C. W., Wieder, W. R., Carey, J. C., Machmuller, M. B., Snoek, B. L., Fang, S., Zhou, G., Allison, S. D., Blair, J. M., Bridgman, S. D., Burton, A. J., Carrillo, Y., Reich, P. B., Clark, J. S., Classen, A. T., Dijkstra, F. A., Elberling, B., Emmett, B. A., Estiarte, M., Frey, S. D., Guo, J., Harte, J., Jiang, L., Johnson, B. R., Kroel-Dulay, G., Larsen, K. S., Laudon, H., Lavallee, J. M., Luo, Y., Lupascu, M., Ma, L. N., Marhan, S., Michelsen, A., Mohan, J., Niu, S., Pendall, E., Penuelas, J., Pfeifer-Meister, L., Poll, C., Reinsch, S., Reynolds, L. L., Schmidt, I. K., Sistla, S., Sokol, N. W., Templer, P. H., Treseder, K. K., Welker, J. M., and Bradford, M. A.: Quantifying global soil carbon losses in response to warming, *Nature*, 540, 104–108, <https://doi.org/10.1038/nature20150>, 2016.
- Darwish, T., Atallah, T., and Fadel, A.: Challenges of soil carbon sequestration in the NENA region, *SOIL*, 4, 225–235, <https://doi.org/10.5194/soil-4-225-2018>, 2018.
- Ding, J. Z., Chen, L. Y., Ji, C. J., Hugelius, G., Li, Y. N., Liu, L., Qin, S. Q., Zhang, B. B., Yang, G. B., Li, F., Fang, K., Chen, Y. L., Peng, Y. F., Zhao, X., He, H. L., Smith, P., Fang, J. Y., and Yang, Y. H.: Decadal soil carbon accumulation across Tibetan permafrost regions, *Nat. Geosci.*, 10, 420–424, <https://doi.org/10.1038/NGEO2945>, 2017.

- Doetterl, S., Berhe, A. A., Arnold, C., Bode, S., Fiener, P., Finke, P., Fuchslueger, L., Griepentrog, M., Harden, J. W., Nadeu, E., Schneckner, J., Six, J., Trumbore, S., Van Oost, K., Vogel, C., and Boeckx, P.: Links among warming, carbon and microbial dynamics mediated by soil mineral weathering, *Nat. Geosci.*, 11, 589–593, <https://doi.org/10.1038/s41561-018-0168-7>, 2018.
- Dontsova, K., Balogh-Brunstad, Z., and Chorover, J.: Plants as drivers of rock weathering, in: *Biogeochemical cycles*, edited by: Dontsova, K., Balogh-Brunstad, Z., Roux, G. L., 33–58, John Wiley Sons, Inc., <https://doi.org/10.1002/9781119413332.ch2>, 2020.
- Frank, J. and Stuanes, A. O.: Short-term effects of liming and vitality fertilization on forest soil and nutrient leaching in a Scots pine ecosystem in Norway, *Forest Ecol. Manag.*, 176, 371–386, [https://doi.org/10.1016/S0378-1127\(02\)00285-2](https://doi.org/10.1016/S0378-1127(02)00285-2), 2003.
- Gandois, L., Perrin, A. S., and Probst, A.: Impact of nitrogenous fertiliser-induced proton release on cultivated soils with contrasting carbonate contents: A column experiment, *Geochim. Cosmochim. Ac.*, 75, 1185–1198, <https://doi.org/10.1016/j.gca.2010.11.025>, 2011.
- Gao, Y., Dang, P., Zhao, Q. X., Liu, J. L., and Liu, J. B.: Effects of vegetation rehabilitation on soil organic and inorganic carbon stocks in the Mu Us Desert, northwest China, *Land Degrad. Dev.*, 29, 1031–1040, <https://doi.org/10.1002/ldr.2832>, 2018.
- Goulding, K.: Soil acidification and the importance of liming agricultural soils with particular reference to the United Kingdom, *Soil Use Manage.*, 32, 390–399, <https://doi.org/10.1111/sum.12270>, 2016.
- Gross, N., Le Bagousse-Pinguet, Y., Liancourt, P., Berdugo, M., Gotelli, N. J., and Maestre, F. T.: Functional trait diversity maximizes ecosystem multifunctionality, *Nat. Ecol. Evol.*, 1, 0132, <https://doi.org/10.1038/s41559-017-0132>, 2017.
- Harley, A. D. and Gilkes, R. J.: Factors influencing the release of plant nutrient elements from silicate rock powders: a geochemical overview, *Nutr. Cycl. Agroecosys.*, 56, 11–36, <https://doi.org/10.1023/A:1009859309453>, 2000.
- Hong, S. B., Gan, P., and Chen, A. P.: Environmental controls on soil pH in planted forest and its response to nitrogen deposition, *Environ. Res.*, 172, 159–165, <https://doi.org/10.1016/j.envres.2019.02.020>, 2019.
- Huang, P., Zhang, J. B., Xin, X. L., Zhu, A. N., Zhang, C. Z., Ma, D. H., Zhu, Q. G., Yang, S., and Wu, S. J.: Proton accumulation accelerated by heavy chemical nitrogen fertilization and its long-term impact on acidifying rate in a typical arable soil in the Huang-Huai-Hai Plain, *J. Integr. Agr.*, 14, 148–157, [https://doi.org/10.1016/S2095-3119\(14\)60750-4](https://doi.org/10.1016/S2095-3119(14)60750-4), 2015.
- Jia, J., Feng, X. J., He, J. S., He, H. B., Lin, L., and Liu, Z. G.: Comparing microbial carbon sequestration and priming in the subsoil versus topsoil of a Qinghai-Tibetan alpine grassland, *Soil Biol. Biochem.*, 104, 141–151, <https://doi.org/10.1016/j.soilbio.2016.10.018>, 2017.
- Jobbágy, E. G. and Jackson, R. B.: The vertical distribution of soil organic carbon and its relation to climate and vegetation, *Ecol. Appl.*, 10, 423–436, <https://doi.org/10.2307/2641104>, 2000.
- Joergensen, R. G.: The fumigation-extraction method to estimate soil microbial biomass: Calibration of the  $k(EC)$  value, *Soil Biol. Biochem.*, 28, 25–31, [https://doi.org/10.1016/0038-0717\(95\)00102-6](https://doi.org/10.1016/0038-0717(95)00102-6), 1996.
- Kuzyakov, Y. and Razavi, B. S.: Rhizosphere size and shape: Temporal dynamics and spatial stationarity, *Soil Biol. Biochem.*, 135, 343–360, <https://doi.org/10.1016/j.soilbio.2019.05.011>, 2019.
- Lal, R.: Soil carbon sequestration impacts on global climate change and food security, *Science*, 304, 1623–1627, <https://doi.org/10.1126/science.1097396>, 2004.
- Lenzowski, N., Mueller, P., Meier, R. J., Liebsch, G., Jensen, K., and Koop-Jakobsen, K.: Dynamics of oxygen and carbon dioxide in rhizospheres of *Lobelia dortmanna* – a planar optode study of belowground gas exchange between plants and sediment, *New Phytol.*, 218, 131–141, <https://doi.org/10.1111/nph.14973>, 2018.
- Le Provost, G., Badenhauer, I., Le Bagousse-Pinguet, Y., Clough, Y., Henckel, L., Violle, C., Bretagnolle, V., Roncoroni, M., Manning, P., and Gross, N.: Land-use history impacts functional diversity across multiple trophic groups, *P. Natl. Acad. Sci. USA*, 117, 1573–1579, <https://doi.org/10.1073/pnas.1910023117>, 2020.
- Li, L., Li, S. M., Sun, J. H., Zhou, L. L., Bao, X. G., Zhang, H. G., and Zhang, F. S.: Diversity enhances agricultural productivity via rhizosphere phosphorus facilitation on phosphorus-deficient soils, *P. Natl. Acad. Sci. USA*, 104, 11192–11196, <https://doi.org/10.1073/pnas.0704591104>, 2007.
- Liu, H. Y., Mi, Z. R., Lin, L., Wang, Y. H., Zhang, Z. H., Zhang, F. W., Wang, H. L., Liu, L. L., Zhu, B., Cao, G. M., Zhao, X. Q., Sanders, N. J., Classen, A. T., Reich, P. B., and He, J. S.: Shifting plant species composition in response to climate change stabilizes grassland primary production, *P. Natl. Acad. Sci. USA*, 115, 4051–4056, <https://doi.org/10.1073/pnas.1700299114>, 2018.
- Liu, S. S., Zhou, L. H., Li, H., Zhao, X., Yang, Y. H., Zhu, Y. K., Hu, F. F., Chen, L. Y., Zhang, P. J., Shen, H. H., and Fang, J. Y.: Shrub encroachment decreases soil inorganic carbon stocks in Mongolian grasslands, *J. Ecol.*, 108, 678–686, <https://doi.org/10.1111/1365-2745.13298>, 2020.
- Liu, X. J., Zhang, Y., Han, W. X., Tang, A. H., Shen, J. L., Cui, Z. L., Vitousek, P., Erisman, J. W., Goulding, K., Christie, P., Fangmeier, A., and Zhang, F. S.: Enhanced nitrogen deposition over China, *Nature*, 494, 459–462, <https://doi.org/10.1038/nature11917>, 2013.
- Liu, Z., Sun, Y. F., Zhang, Y. Q., Feng, W., Lai, Z. R., and Qin, S. G.: Soil microbes transform inorganic carbon into organic carbon by dark fixation pathways in desert soil, *J. Geophys. Res.-Biogeo.*, 126, e2020JG006047, <https://doi.org/10.1029/2020JG006047>, 2021.
- Mi, N., Wang, S. Q., Liu, J. Y., Yu, G. R., Zhang, W. J., and Jobbaagy, E.: Soil inorganic carbon storage pattern in China, *Glob. Change Biol.*, 14, 2380–2387, <https://doi.org/10.1111/j.1365-2486.2008.01642.x>, 2008.
- Monger, H. C., Kraimer, R. A., Khresat, S., Cole, D. R., Wang, X. J., and Wang, J. P.: Sequestration of inorganic carbon in soil and groundwater, *Geology*, 43, 375–378, <https://doi.org/10.1130/G36449.1>, 2015.
- Moorhead, D. L. and Sinsabaugh, R. L.: A theoretical model of litter decay and microbial interaction, *Ecol. Monogr.*, 76, 151–174, [https://doi.org/10.1890/0012-9615\(2006\)076\[0151:ATMOLD\]2.0.CO;2](https://doi.org/10.1890/0012-9615(2006)076[0151:ATMOLD]2.0.CO;2), 2006.
- Oelkers, E. H., Benning, L. G., Lutz, S., Mavromatis, V., Pearce, C. R., and Plummer, O.: The efficient long-term inhibition of forsterite dissolution by common soil bacteria and fungi at Earth

- surface conditions, *Geochim. Cosmochim. Ac.*, 168, 222–235, <https://doi.org/10.1016/j.gca.2015.06.004>, 2015.
- Pan, J. X., Zhang, L., He, X. M., Chen, X. P., and Cui, Z. L.: Long-term optimization of crop yield while concurrently improving soil quality, *Land Degrad. Dev.*, 30, 897–909, <https://doi.org/10.1002/ldr.3276>, 2019.
- Pan, J. X., Wang, J. S., Zhang, R. Y., Tian, D. S., Cheng, X. L., Wang, S., Chen, C., Yang, L., and Niu, S. L.: Microaggregates regulated by edaphic properties determine the soil carbon stock in Tibetan alpine grasslands, *Catena*, 206, 105570, <https://doi.org/10.1016/j.catena.2021.105570>, 2021.
- Peng, S., Ding, Y., Liu, W., and Li, Z.: 1 km monthly temperature and precipitation dataset for China from 1901 to 2017, *Earth Syst. Sci. Data*, 11, 1931–1946, <https://doi.org/10.5194/essd-11-1931-2019>, 2019.
- Prietz, J., Zimmermann, L., Schubert, A., and Christophel, D.: Organic matter losses in German Alps forest soils since the 1970s most likely caused by warming, *Nat. Geosci.*, 9, 543, <https://doi.org/10.1038/NGEO2732>, 2016.
- Raza, S., Miao, N., Wang, P. Z., Ju, X. T., Chen, Z. J., Zhou, J. B., and Kuzyakov, Y.: Dramatic loss of inorganic carbon by nitrogen-induced soil acidification in Chinese croplands, *Glob. Change Biol.*, 26, 3738–3751, <https://doi.org/10.1111/gcb.15101>, 2020.
- Rey, A.: Mind the gap: non-biological processes contributing to soil CO<sub>2</sub> efflux, *Glob. Change Biol.*, 21, 1752–1761, <https://doi.org/10.1111/gcb.12821>, 2015.
- Rowley, M. C., Grand, S., and Verrecchia, E. P.: Calcium-mediated stabilisation of soil organic carbon, *Biogeochemistry*, 137, 27–49, <https://doi.org/10.1007/s10533-017-0410-1>, 2018.
- Rumpel, C., Chabbi, A., and Marschner, B.: Carbon storage and sequestration in subsoil horizons: Knowledge, gaps and potentials, in: *Recarbonization of the biosphere: ecosystems and the global carbon cycle*, edited by: Lal, R., Lorenz, K., Huttel, R. F., Uwe Schneider, B., and von Braun, J., 445–464, Springer, Heidelberg, Germany, [https://doi.org/10.1007/978-94-007-4159-1\\_20](https://doi.org/10.1007/978-94-007-4159-1_20), 2012.
- Sartori, F., Lal, R., Ebinger, M. H., and Eaton, J. A.: Changes in soil carbon and nutrient pools along a chronosequence of poplar plantations in the Columbia Plateau, Oregon, USA, *Agr. Ecosyst. Environ.*, 122, 325–339, <https://doi.org/10.1016/j.agee.2007.01.026>, 2007.
- Song, X. D., Yang, F., Wu, H. Y., Zhang, J., Li, D. C., Liu, F., Zhao, Y. G., Yang, J. L., Ju, B., Cai, C. F., Huang, B. A., Long, H. Y., Lu, Y., Sui, Y. Y., Wang, Q. B., Wu, K. N., Zhang, F. R., Zhang, M. K., Shi, Z., Ma, W. Z., Xin, G., Qi, Z. P., Chang, Q. R., Ci, E., Yuan, D. G., Zhang, Y. Z., Bai, J. P., Chen, J. Y., Chen, J., Chen, Y. J., Dong, Y. Z., Han, C. L., Li, L., Liu, L. M., Pan, J. J., Song, F. P., Sun, F. J., Wang, D. F., Wang, T. W., Wei, X. H., Wu, H. Q., Zhao, X., Zhou, Q., and Zhang, G. L.: Significant loss of soil inorganic carbon at the continental scale, *Natl. Sci. Rev.*, 9, nwab120, <https://doi.org/10.1093/nsr/nwab120>, 2022.
- Tang, C., Unkovich, M. J., and Bowden, J. W.: Factors affecting soil acidification under legumes. III. Acid production by N<sub>2</sub>-fixing legumes as influenced by nitrate supply, *New Phytol.*, 143, 513–521, <https://doi.org/10.1046/j.1469-8137.1999.00475.x>, 1999.
- Tatti, E., McKew, B. A., Whitby, C., and Smith, C. J.: Simultaneous DNA-RNA extraction from coastal sediments and quantification of 16S rRNA genes and transcripts by real-time PCR, *J. Vis. Exp.*, 112, e54067, <https://doi.org/10.3791/54067>, 2016.
- Todd-Brown, K. E. O., Randerson, J. T., Post, W. M., Hoffman, F. M., Tarnocai, C., Schuur, E. A. G., and Allison, S. D.: Causes of variation in soil carbon simulations from CMIP5 Earth system models and comparison with observations, *Biogeosciences*, 10, 1717–1736, <https://doi.org/10.5194/bg-10-1717-2013>, 2013.
- van Hees, P., Rosling, A., Essen, S., Godbold, D. L., Jones, D. L., and Finlay, R. D.: Oxalate and ferrioxalate exudation by the extramatrical mycelium of an ectomycorrhizal fungus in symbiosis with *Pinus sylvestris*, *New Phytol.*, 169, 367–377, <https://doi.org/10.1111/j.1469-8137.2005.01600.x>, 2006.
- Ven, A., Verlinden, M. S., Fransen, E., Olsson, P. A., Verbruggen, E., Wallander, H., and Vicca, S.: Phosphorus addition increased carbon partitioning to autotrophic respiration but not to biomass production in an experiment with *Zea mays*, *Plant Cell Environ.*, 43, 2054–2065, <https://doi.org/10.1111/pce.13785>, 2020.
- Vicca, S., Goll, D. S., Hagens, M., Hartmann, J., Janssens, I. A., Neubeck, A., Penuelas, J., Poblador, S., Rijnders, J., Sardans, J., Struyf, E., Swoboda, P., van Groenigen, J. W., Vienne, A., and Verbruggen, E.: Is the climate change mitigation effect of enhanced silicate weathering governed by biological processes?, *Glob. Change Biol.*, 28, 711–726, <https://doi.org/10.1111/gcb.15993>, 2022.
- Wang, B., Bao, Q., Hoskins, B., Wu, G. X., and Liu, Y. M.: Tibetan plateau warming and precipitation changes in East Asia, *Geophys. Res. Lett.*, 35, L14702, <https://doi.org/10.1029/2008GL034330>, 2008.
- Wang, G. X., Qian, J., Cheng, G. D., and Lai, Y. M.: Soil organic carbon pool of grassland soils on the Qinghai-Tibetan Plateau and its global implication, *Sci. Total. Environ.*, 291, 207–217, [https://doi.org/10.1016/S0048-9697\(01\)01100-7](https://doi.org/10.1016/S0048-9697(01)01100-7), 2002.
- Wang, J. P., Wang, X. J., Zhang, J., and Zhao, C. Y.: Soil organic and inorganic carbon and stable carbon isotopes in the Yanqi Basin of northwestern China, *Eur. J. Soil Sci.*, 66, 95–103, <https://doi.org/10.1111/ejss.12188>, 2015.
- Wild, B., Imfeld, G., and Daval, D.: Direct measurement of fungal contribution to silicate weathering rates in soil, *Geology*, 49, 1055–1058, <https://doi.org/10.1130/G48706.1>, 2021.
- Xiao, L. L., Lian, B., Hao, J. C., Liu, C. Q., and Wang, S. J.: Effect of carbonic anhydrase on silicate weathering and carbonate formation at present day CO<sub>2</sub> concentrations compared to primordial values, *Sci. Rep.-UK*, 5, 7733, <https://doi.org/10.1038/srep07733>, 2015.
- Yang, R. M. and Yang, F.: Impacts of *Spartina alterniflora* invasion on soil inorganic carbon in coastal wetlands in China, *Soil Sci. Soc. Am. J.*, 84, 844–855, <https://doi.org/10.1002/saj2.20073>, 2020.
- Yang, Y. H., Fang, J. Y., Ji, C. J., Ma, W. H., Su, S. S., and Tang, Z. Y.: Soil inorganic carbon stock in the Tibetan alpine grasslands, *Global Biogeochem. Cy.*, 24, GB4022, <https://doi.org/10.1029/2010GB003804>, 2010.
- Yang, Y. H., Ji, C. J., Ma, W. H., Wang, S. F., Wang, S. P., Han, W. X., Mohammad, A., and Smith, P.: Significant soil acidification across northern China's grasslands during 1980s–2000s, *Glob. Change Biol.*, 18, 2292–2300, <https://doi.org/10.1111/j.1365-2486.2012.02694.x>, 2012.
- Yost, J. L. and Hartemink, A. E.: How deep is the soil studied – an analysis of four soil science journals, *Plant Soil*, 452, 5–18, <https://doi.org/10.1007/s11104-020-04550-z>, 2020.

- Yu, G. R., Jia, Y. L., He, N. P., Zhu, J. X., Chen, Z., Wang, Q. F., Piao, S. L., Liu, X. J., He, H. L., Guo, X. B., Wen, Z., Li, P., Ding, G. A., and Goulding, K.: Stabilization of atmospheric nitrogen deposition in China over the past decade, *Nat. Geosci.*, 12, 424–429, <https://doi.org/10.1038/s41561-019-0352-4>, 2019.
- Zamanian, K. and Kuzyakov, Y.: Contribution of soil inorganic carbon to atmospheric CO<sub>2</sub>: More important than previously thought, *Glob. Change Biol.*, 25, E1–E3, <https://doi.org/10.1111/gcb.14463>, 2019.
- Zamanian, K., Pustovoytov, K., and Kuzyakov, Y.: Pedogenic carbonates: Forms and formation processes, *Earth-Sci. Rev.*, 157, 1–17, <https://doi.org/10.1016/j.earscirev.2016.03.003>, 2016.
- Zamanian, K., Zarebanadkouki, M., and Kuzyakov, Y.: Nitrogen fertilization raises CO<sub>2</sub> efflux from inorganic carbon: A global assessment, *Glob. Change Biol.*, 24, 2810–2817, <https://doi.org/10.1111/gcb.14148>, 2018.
- Zaharescu, D. G., Burghilea, C. I., Dontsova, K., Reinhard, C. T., Chorover, J., and Lybrand, R.: Biological weathering in the terrestrial system: An evolutionary perspective, in: *Biogeochemical Cycles: Ecological Drivers and Environmental Impact*, edited by: Dontsova, K., Balogh-Brunstad, Z., and Le Roux, G., AGU, 1–32, <https://doi.org/10.1002/9781119413332.ch1>, 2020.
- Zang, H. D., Blagodatskaya, E., Wen, Y., Xu, X. L., Dyckmans, J., and Kuzyakov, Y.: Carbon sequestration and turnover in soil under the energy crop *Miscanthus*: repeated C-13 natural abundance approach and literature synthesis, *GCB Bioenergy*, 10, 262–271, <https://doi.org/10.1111/gcbb.12485>, 2018.
- Zhou, Z., Li, Z., Chen, K., Chen, Z., Zeng, X., Yu, H., Guo, S., Shangguan, Y., Chen, Q., Fan, H., Tu, S., He, M., and Qin, Y.: Changes in soil physicochemical properties and bacterial communities at different soil depths after long-term straw mulching under a no-till system, *SOIL*, 7, 595–609, <https://doi.org/10.5194/soil-7-595-2021>, 2021.